



# Direct dynamics determination of the reaction pathways for decomposition of the cross-linked epoxy resin constituent $\text{CH}_3\text{—NH—CH=CH—CH}_3$

Li Yang, Rui Sun, William L. Hase\*

Department of Chemistry and Biochemistry, Texas Tech University, Lubbock, TX 79409, United States

## ARTICLE INFO

### Article history:

Received 13 October 2011

Received in revised form 25 October 2011

Accepted 3 November 2011

Available online 17 November 2011

### Keywords:

Direct dynamics simulation

Epoxy resin decomposition

Unimolecular decomposition mechanisms

## ABSTRACT

Direct dynamics simulations at the MP2/6-31+G\* level of theory were performed to study the unimolecular decomposition of the epoxy resin constituent  $\text{CH}_3\text{—NH—CH=CH—CH}_3$  for the hyperthermal temperatures of 3500–5500 K. At these temperatures 33 different primary decomposition pathways were found, with C–N bond dissociation to form  $\text{CH}_3 + \text{NH—CH=CH—CH}_3$  the most important path. In addition, during the 5.1 ps integration time of the simulations, an additional 15 secondary decomposition pathways were observed. The unimolecular products of the simulations are in qualitative agreement with those observed in the high temperature decomposition of a cross-linked epoxy resin for which  $\text{CH}_3\text{—NH—CH=CH—CH}_3$  is a constituent.

© 2011 Elsevier B.V. All rights reserved.

## 1. Introduction

Crosslinked epoxy resins, resulting from open-ring copolymerization of epoxy resins by “hardener” compounds, are a major class of thermosetting polymers. They often are superior as compared to linear polymers, for properties such as high modulus and fracture strength, low creep and high-temperature performances, and thus widely serve as coatings, adhesives, composites, etc. in the electronics and aerospace industries [1–4]. On the other hand, layered double hydroxides (LDHs) are a family of layered crystals, which can be modified by intercalating organic ions between the lamellas and can be profitably used as nanofillers for the synthesis of nanocomposites [5–8]. Inorganic/organic nanocomposites typically have better mechanical, thermal, optical and physico-chemical properties than the pristine polymer. It has been reported that exfoliated nanocomposites formed by LDH-aminobenzoate and epoxy showed significant enhancement in mechanical and thermal properties; e.g., increased tensile modulus, lower coefficient of thermal expansion and higher decomposition temperature [9].

Extensive applications of cross-linked epoxy resins continue to be important for a variety of studies. A detailed understanding of the resins' decomposition pathways is necessary to better interpret experiment and to have a more accurate description of epoxy nanocomposites. There have been experimental studies on the thermal degradation of bisphenol-a diglycidyl ether cured with ethylene diamine, but apparently there are no complementary theoretical studies for such resins [10].

Computer simulations provide an excellent route to study these polymer networks. While on one hand, they can reduce trial and

error experimentation; on the other hand, they provide insightful information which is often difficult to extract from experiments. In the current paper, direct dynamics simulations [11,12] are reported for the gas-phase unimolecular decomposition of the cross-linked epoxy resin constituent,  $\text{CH}_3\text{—NH—CH=CH—CH}_3$ , [10] using the MP2/6-31+G\* level of theory. The primary and secondary isomerization and dissociation unimolecular pathways for this model molecule are established.

## 2. Computational methodology

The simulations were performed using direct dynamics in which the technology of classical trajectory calculations is coupled with electronic structure theory. In this manner, the gradient, energy and possibly Hessian [13,14] needed to calculate the trajectory come directly from an electronic structure theory, without the need for an analytic potential energy function. To initialize the trajectories, the phase space of the reactant molecule is excited randomly at fixed energy  $E$  to form a microcanonical ensemble [15].

The simulations of  $\text{CH}_3\text{—NH—CH=CH—CH}_3$  unimolecular decomposition were performed by exciting microcanonical ensembles of molecules so that their temperatures ( $E = sk_B T$ , where  $s$  is the number of vibrational modes for the molecule) were 3500, 4000, 4500, 5000, and 5500 K. The software package consisting of the chemical dynamics computer program VENUS [16,17] interfaced with the NWChem [18] electronic structure computer program was used for the simulations. A sixth-order symplectic integration algorithm [19,20] was used to propagate each trajectory with a time step of 0.3 fs. A total of 100 trajectories were calculated for each temperature. The simulations were performed by direct dynamics using the MP2/6-31+G\* electronic structure theory. The trajectories with  $T$  of 3500–5000 K were integrated for  $t_{max}$

\* Corresponding author.

E-mail address: [bill.hase@ttu.edu](mailto:bill.hase@ttu.edu) (W.L. Hase).

of 5.1 ps or until a unimolecular reaction occurred. The 5500 K trajectories were integrated with  $t_{max} = 3.3$  ps. The total energy of the trajectories was conserved to within 0.2 kcal/mol. The primary and secondary unimolecular decomposition pathways for the molecules were determined by animating the trajectories.

The above temperatures of 3500–5500 K, based on the total energies  $E = sk_B T$ , are classical. It is of interest to determine the quantum temperatures for these energies and see if they are significantly different. This latter temperature is found by first subtracting the  $\text{CH}_3\text{-NH-CH=CH-CH}_3$  zero point energy from the total energy to obtain the quantum vibrational energy  $E_q(T)$  for  $\text{CH}_3\text{-NH-CH=CH-CH}_3$ . A thermal energy  $\varepsilon_i(T)$ , at quantum temperature  $T$ , is then added to each of the vibrational modes of  $\text{CH}_3\text{-NH-CH=CH-CH}_3$  to match this quantum vibrational energy; i.e.

$$E_q(T) = \sum \varepsilon_i(T) = sk_B T - E_{zpe} \quad (1)$$

where

$$\varepsilon_i(T) = hv / [\exp(hv/k_B T) - 1] \quad (2)$$

The resulting quantum temperatures are similar to the classical temperatures and 3338, 3863, 4384, 4901, and 5415 K, respectively, for the classical temperatures of 3500, 4000, 4500, 5000, and 5500 K.

### 3. Simulation results

Our goal is to determine the types and probabilities of different unimolecular dissociation pathways for the repeat unit of epoxy resins (Fig. 1) to gain insight into the importance of different types of decompositions. A total of 33 different primary decomposition pathways were observed, and mechanistic analyses of these pathways and their relationship to experiment are presented here. Some of the primary reaction products undergo secondary decomposition during the limited time of the trajectory integrations, and these secondary decompositions are also identified. It is understood that, if the trajectories were run for longer times, more secondary dissociations will be observed.

#### 3.1. Primary dissociation pathways

The number of trajectories, which decomposed by each of the different primary decomposition pathways, is listed in Table 1. The reactions are classified by type in the following.

##### 3.1.1. Reactions producing the $\text{CH}_3$ radical

As shown in Table 1, all bonds between two heavy atoms possibly break. The most likely event is C–N bond rupture to form the radicals  $\cdot\text{CH}_3$  and  $\cdot\text{NH-CH=CH-CH}_3$  (Path 1) with a probability

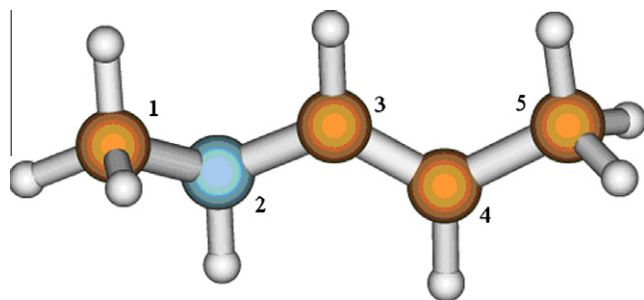
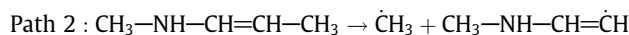
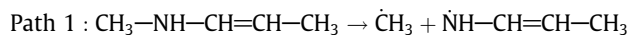


Fig. 1. Structure of  $\text{CH}_3\text{-NH-CH=CH-CH}_3$ , the molecule considered for the direct dynamics unimolecular decomposition studies. The atom labels are for the heavy atoms.

of at least 50% within the 3500–5500 K exciting temperature range. Path 2 is rare event and only takes place at the higher temperatures with very little probability.



##### 3.1.2. Reactions producing $\text{H}_2$

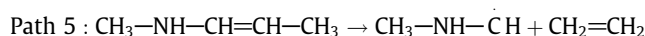
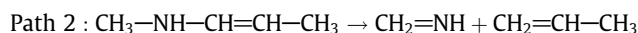
It is possible for any two hydrogen atoms on the backbone of  $\text{CH}_3\text{-NH-CH=CH-CH}_3$  to interact and form  $\text{H}_2$  as shown in Table 1. These  $\text{H}_2$  formation pathways become important for temperatures of 4500 K and higher.

##### 3.1.3. Reactions producing $\text{CH}_4$

The reactions forming the  $\text{CH}_4$  molecule only take place at the high temperatures of 5000 and 5500 K. The other products are also closed shell, singlet state species. Methane is primarily formed from the  $\text{CH}_3$  group bonded to the N-atom, with the H-atom migrating from one of the other heavy atoms. Only for one of the five  $\text{CH}_4$  forming reactions is the  $\text{CH}_3$  group bonded to the C-atom. One of these reactions forms 3 products, i.e.  $\text{H}_2$  and  $\text{NH=C=C=CH}_2$  in addition to  $\text{CH}_4$  [21].

##### 3.1.4. Reactions producing an amine

Four reactions occur to form amine products; i.e.



The first and second paths involve N2–C3 bond dissociation and only differ by the H migration. For Path 1, a H-atom shifts from C4 to N2 and for Path 2 this shift is from C1 to C3, forming methylamine and methyleneimine, respectively. Path 3 includes C3–C4 bond breaking which is concerted with H-atom shifting from C5 to C3, to form  $\text{CH}_3\text{-N=CH}_2$  and  $\text{CH}_2=\text{CH}_2$ . Path 4 is a N2–C3 bond dissociation between N2 and C3 forming two radicals. It occurred at all temperatures except the lowest temperature of 3500 K. The remaining reactions occurred at the higher temperatures.

##### 3.1.5. Reactions producing the $\text{CH}_2$ radical

For the two reactions producing the  $\text{CH}_2$  radical, migration of a H-atom from one of the ending  $\text{CH}_3$  groups to either N2 or C4 first takes place, and then there is respective breakage of C1–N2 or C4–C5 to form two alkene molecules.

#### 3.2. Isomerization pathways

Ten isomerization pathways occur within the 3500–5500 K temperature range as shown in Table 1. The isomerizations via H-atom transfer, to form  $\text{CH}_3\text{-N=CH-CH}_2\text{-CH}_3$  and  $\text{CH}_3\text{-NH-CH}_2\text{-CH=CH}_2$ , are the most important. The first path involves H-atom shifting from N2 to C4, forming a C3–C4 single bond and N2–C3 double bond. For Path 2, migration of a H-atom from C5 to C3 leads to a C4–C5 double bond and turns the C3–C4 double bond into a single bond.

There are three  $\text{CH}_3$  migration pathways; i.e.

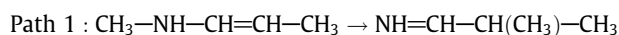
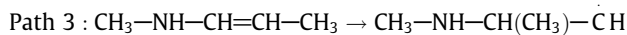
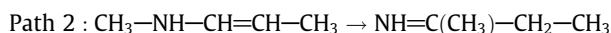


**Table 1**  
Number of reactions for the different unimolecular pathways.

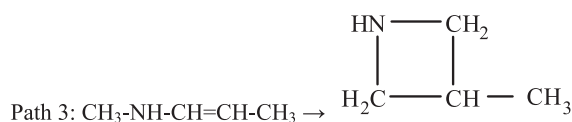
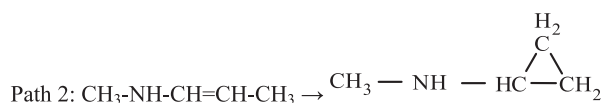
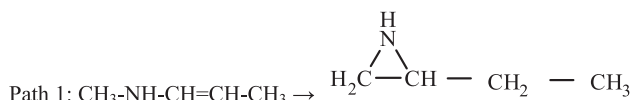
Pathways	Temp (K)				
	3500	4000	4500	5000	5500
$\dot{\text{C}}\text{H}_3 + \dot{\text{N}}\text{H}-\text{CH}=\text{CH}-\text{CH}_3$	3	10	27	38	52
$\text{CH}_3 + \text{CH}_3-\text{NH}-\dot{\text{C}}\text{H}=\dot{\text{C}}\text{H}$			1	1	3
$\text{H}_2 + \dot{\text{C}}\text{H}-\text{NH}-\text{CH}=\text{CH}-\text{CH}_3$		1		2	3
$\text{H}_2 + \text{CH}_3-\text{N}=\text{C}=\dot{\text{C}}\text{H}-\text{CH}_3$			1		1
$\text{H}_2 + \text{CH}_3-\text{NH}-\dot{\text{C}}\text{H}=\text{C}=\text{CH}_2$					1
$\text{H}_2 + \dot{\text{C}}\text{H}_2-\text{NH}-\dot{\text{C}}=\text{CH}-\text{CH}_3$			2	3	1
$\text{H}_2 + \text{CH}_2=\text{N}-\dot{\text{C}}\text{H}=\text{CH}-\text{CH}_3$				3	
$\text{H}_2 + \text{CH}_3-\text{NH}-\dot{\text{C}}\equiv\text{C}-\text{CH}_3$				1	2
$\text{H}_2 + \text{CH}_2=\text{NH} + \text{HC}\equiv\text{C}-\text{CH}_3$					1
$\text{CH}_4 + \text{N}\equiv\text{C}-\text{CH}_2-\dot{\text{C}}\text{H}_3$				2	1
$\text{CH}_4 + \text{CH}_3-\text{NH}-\dot{\text{C}}\equiv\text{CH}$				2	1
$\text{HC}=\text{N}-\dot{\text{C}}\text{H}-\text{CH}_3$				2	1
$\text{CH}_4 + \text{H}_2 + \text{NH}=\text{C}=\text{C}=\text{CH}_2$					1
$\text{CH}_4 + \text{NH}=\text{C}=\dot{\text{C}}\text{H}-\text{CH}_3$					1
$\text{CH}_3-\dot{\text{N}}\text{H} + \dot{\text{C}}\text{H}=\text{CH}-\text{CH}_3$		3	1	4	3
$\text{CH}_3-\text{NH}_2 + \text{HC}\equiv\text{C}-\text{CH}_3$			4	4	4
$\text{CH}_2=\text{NH} + \text{CH}_2=\text{CH}-\text{CH}_3$				1	3
$\text{CH}_3-\text{N}=\text{CH}_2 + \text{CH}_2=\text{CH}_2$				1	
$\text{CH}_3-\text{NH}-\dot{\text{C}}\text{H} + \text{CH}_2=\text{CH}_2$				1	
$\dot{\text{C}}\text{H}_2 + \text{NH}_2-\text{CH}=\text{CH}-\text{CH}_3$					3
$\dot{\text{C}}\text{H}_2 + \text{CH}_3-\text{NH}-\text{CH}=\text{CH}_2$					2
$\text{CH}_3-\text{N}=\text{CH}-\text{CH}_2-\dot{\text{C}}\text{H}_3$	2	2	4	9	2
$\text{CH}_3-\text{NH}-\text{CH}_2-\dot{\text{C}}\text{H}=\text{CH}_2$			5	1	7
$\text{NH}=\text{CH}-\text{CH}(\text{CH}_3)-\dot{\text{C}}\text{H}_3$	1		1	1	1
$\text{NH}=\text{C}(\text{CH}_3)-\text{CH}_2-\dot{\text{C}}\text{H}_3$		1			
$\text{CH}_3-\text{NH}-\text{CH}(\text{CH}_3)-\dot{\text{C}}\text{H}$					1
$\text{CH}_3-\text{NH}-\text{HC}=\text{CH}_2$				3	3
$\text{H}_2$					
$\text{CH}_3-\text{NH}-\text{HC}=\text{CH}_2$		2		2	
$\text{H}_2\text{C}-\text{CH}=\text{CH}_2-\text{CH}_3$				1	
$\text{HN}-\text{CH}_2$					1
$\text{H}_2\text{C}-\text{CH}-\text{CH}_3$					
$\text{CH}_3-\text{NH}-\text{C}-\text{CH}_2-\text{CH}_3$			1		2
$\text{CH}_3-\text{NH}-\text{CH}_2-\text{C}-\text{CH}_3$				1	
$\text{CH}_3-\dot{\text{N}}-\text{CH}_2-\dot{\text{C}}\text{H}-\text{CH}_3$			1		

<sup>a</sup>100 Trajectories were calculated for each temperature.



The  $\text{CH}_3$  group bonding to N shifts to C4 or C3, respectively, for Paths 1 and 2, leading to the respective  $\text{N}=\text{C}$  double bond products  $\text{NH}=\text{CH}-\text{CH}(\text{CH}_3)-\text{CH}_3$  and  $\text{NH}=\text{C}(\text{CH}_3)-\text{CH}_2-\text{CH}_3$ . For Path 3, the  $\text{CH}_3$  group bonding to C4 migrates to C3 forming the  $\text{CH}_3-\text{NH}-\text{CH}(\text{CH}_3)-\dot{\text{C}}\text{H}$  product.

Three paths involve  $\text{CH}_3-\text{NH}-\text{CH}=\text{CH}-\text{CH}_3$  isomerization to form three- or four-membered rings; i.e.



For Path 1, the  $\text{CH}_3$  group migration to C3 is associated with concerted C1–C3 bond formation and a H shifting to C4, to form the C1–N2–C3 three-membered ring. Similarly for Path 2, the  $\text{CH}_3$  group bonding to C4 shifts to C3 accompanied by C3–C4–C5 ring closure and a H shifting to C4, to form the three-membered

ring product. For Path 3, the CH<sub>3</sub> group bonding to N2 migrates to C4, leading to C1–C4 bond formation and then closing the C1–N2–C3–C4 four-membered ring with H shifting to C3.

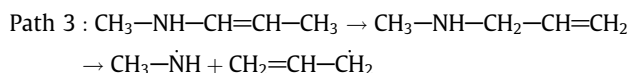
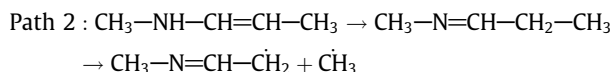
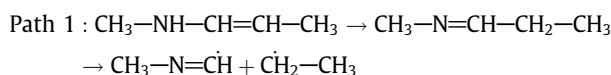
There are two pathways with H-atom migration at the C=C double bond. A H-atom on C3 or H-atom on C4 shifts, respectively, to C4 and C3 to form radical products. Another pathway consists of H-atom transfer from N to C3 and also forms a radical product. These three radical products can further dissociate to secondary dissociation products.

### 3.3. Secondary dissociation pathways

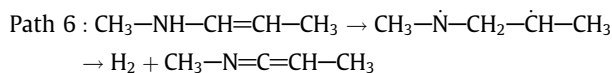
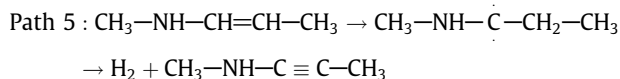
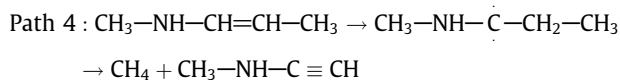
#### 3.2.1. Secondary dissociations from primary isomerization products

The secondary dissociations only occur at the higher temperatures of 4500–5500 K and the number of dissociations increase with increasing temperature. Within  $t_{\max}$ , the maximum integration time, nine secondary dissociation pathways are found from the primary isomerization products.

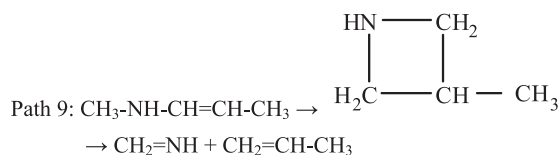
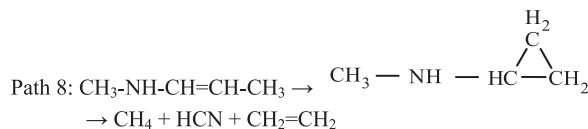
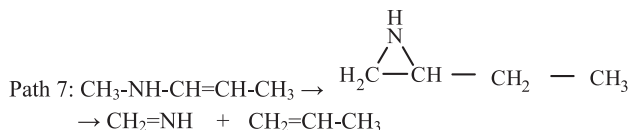
Radical products were formed from the isomerization products, through direct bond rupture and without H-atom migration, via Paths 1, 2 and 3 below:



Two radical isomerization products further dissociate to molecular products by Paths 4, 5 and 6. Paths 4 and 5 start from the same radical isomerization product and then dissociate to different secondary products, i.e. CH<sub>4</sub> + CH<sub>3</sub>–NH–C≡CH and H<sub>2</sub> + CH<sub>3</sub>–NH–C≡C–CH<sub>3</sub>.

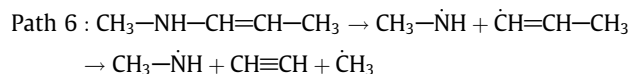
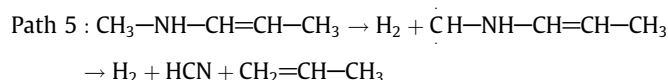
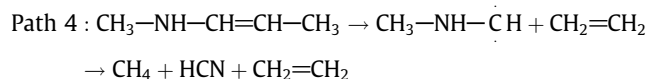
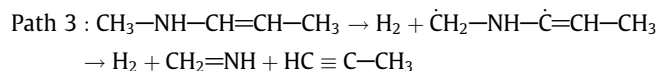
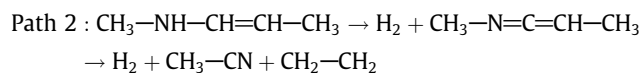
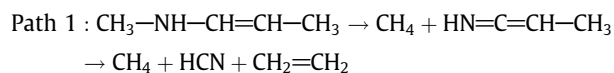


The isomerization ring products further dissociated into molecular species. For Path 7 the N–C and C–C bonds of the three-membered ring break and at the same time a H-atom migrates from C4 to C3 to form two double bond products, i.e., CH<sub>2</sub>=NH and CH<sub>2</sub>=CH–CH<sub>3</sub>. For Path 8 the two C–C bonds of the three-membered ring break to form CH<sub>2</sub>=CH<sub>2</sub>. This occurs concurrently with C1–N2 bond rupture yielding the reaction products CH<sub>4</sub> and HCN. The N–C and C–C bonds rupture in the four-membered ring for Path 9, yielding the two double bonds products CH<sub>2</sub>=NH and CH<sub>2</sub>=CH–CH<sub>3</sub>.



#### 3.2.2. Secondary dissociations from primary dissociation products

Six secondary dissociations occur from the primary dissociation products. For Paths 1 and 2, concomitant with H-atom migration, primary molecular products further dissociate into different molecular products. For Paths 3, 4, and 5 the primary products are radicals, which further dissociate to singlet products, accompanied by H-atom transfer. Path 6 forms radical primary products and then one of these products undergoes further dissociation without H-atom migration.



## 4. Comparison with experiment

Our model study is similar to the experimental work of Grassie and co-workers [10]. Their experimental system is thermal degradation of a commercial epoxy resin prepared by reaction of 2,2-bis-(4'-hydroxyl phenyl)propane (bisphenol-A) with 1-chloro-2,3-epoxy propane (epichlorhydrin) and cross-lined (cured) with ethylene diamine. The following products were identified by IR and mass spectrometry; i.e. hydrogen and methane, ethane, propene, ammonia, methylamine with a trace of trimethylamine, water, phenol, cresols, 4-isopropyl phenol, and other trace products.

Although the experimental system is a very large polymer and more complex than our model system, in examining the decomposition products of our model system it is seen that several important simulation products are also important experimental products. They are hydrogen, methane, and methylamine. The principal products observed experimentally include hydrogen and methane, which are also observed as primary products in our simulations. For the experimental

system, the N-atom is bonded to the  $-\text{CH}_2-\text{CH}_2-$  group and N–C dissociation is expected to yield ethane as a reaction product. For our model system the N-atom connects to a  $\text{CH}_3$  group.  $\text{CH}_3$  radicals are a dominant product in our simulations, which is very similar to the experimental observation of ethane as a principal product.

The time scale of our simulations is rather limited at 5.1 ps. It is possible that further fragmentation of the  $\text{CH}_3-\text{NH}-\text{CH}=\text{CH}-\text{CH}_3$  molecule could take place on a longer time scale. In this work, we find many isomerization pathways which are not measured experimentally. Overall, the simulation decomposition products are in qualitative agreement with the experimental results, although there are differences between the model and experimental systems.

The simulations reported here were performed for the 3500–5500 K temperature range. As shown in a recent study [22], by determining the unimolecular rate constant for a primary decomposition path versus temperature it is possible to determine the Arrhenius parameters  $A$  and  $E_a$ , i.e.  $k(T) = A \exp(-E_a/k_B T)$ , for the pathway. In this manner, the pathways with the lowest activation energies may be determined to assist in establishing the important primary decomposition pathways at lower temperatures.

### Acknowledgments

This material is based on work supported by the Office of Naval Research under Award No. N00014-09-1-0626 and by the Robert A. Welch Foundation under Grant No. D-0005. The Hrothgar computer cluster at Texas Tech University, within the High Performance Computing Center and under the direction of Philip W. Smith, was used for the simulations reported here.

### References

- [1] H. Liu, A. Uhlherr, M.K. Bannister, *Polymer* 45 (2004) 2051.
- [2] P. Boinard, W.M. Banks, R.A. Pethrick, *Polymer* 46 (2005) 2218.
- [3] Y. Ni, S. Zheng, K. Nie, *Polymer* 45 (2004) 5557.
- [4] C. Wu, W. Xu, *Polymer* 47 (2006) 6004.
- [5] M. Alexandre, P. Dubios, *Mater. Sci. Eng. R.* 28 (2000) 1.
- [6] T. Pinnavaia, *J. Sci.* 220 (1983) 365.
- [7] E.P. Giannelis, R. Krishnamoorti, E. Manias, *Adv. Polym. Sci.* 138 (1999) 107.
- [8] M. Zammarano, M. Franceschi, S. Bellayer, J.W. Gilman, S. Meriani, *Polymer* 46 (2005) 9314.
- [9] C.H. Tseng, H.B. Hsueh, C.Y. Chen, *Compos. Sci. Technol.* 67 (2007) 2350.
- [10] N. Grassie, M.I. Guy, *Polym. Degrad. Stabil.* 14 (1986) 125.
- [11] K. Bolton, W.L. Hase, G.H. Peslherbe, Direct dynamics simulations of reactive systems, in: D.L. Thompson (Ed.), *Multidimensional Molecular Dynamics Methods*, World Scientific Publishing, Inc., London, 1998, pp. 143–189.
- [12] L. Sun, W.L. Hase, *Rev. Comput. Chem.* 19 (2003) 79.
- [13] U. Lourderaj, K. Song, T.L. Windus, Y. Zhuang, W.L. Hase, *J. Chem. Phys.* 126 (2007) 044105.
- [14] H. Wu, M. Rahman, J. Wang, U. Lourderaj, W.L. Hase, Y. Zhuang, *J. Chem. Phys.* 133 (2010) 074101.
- [15] G.H. Peslherbe, H. Wang, W.L. Hase, *Adv. Chem. Phys.* 105 (1999) 171.
- [16] W.L. Hase, R.J. Duchovic, X. Hu, A. Domornicki, K.F. Lim, D.H. Lu, G.H. Peslherbe, S.R. Swamy, S.R. Vande Linde, A. Varandas, R.J. Wolfe, *Quant. Chem. Prog. Exchange (QCPE) Bull.* 16 (1996) 671.
- [17] X. Hu, W.L. Hase, T.J. Pirraglia, *Comput. Chem.* 12 (1992) 1014–1024.
- [18] E.J. Bylaska, W.A. de Jong, N. Govind, K. Kowalski, T.P. Straatsma, M. Valiev, D. Wang, E. Apra, T.L. Windus, J. Hammond, P. Nichols, S. Hirata, M.T. Hackler, Y. Zhao, P.-D. Fan, R.J. Harrison, M. Dupuis, D.M.A. Smith, J. Nieplocha, V. Tipparaju, M. Krishnan, Q. Wu, T. Van Voorhis, A.A. Auer, M. Nooijen, E. Brown, G. Cisneros, G.I. Fann, H. Fruchtl, J. Garza, K. Hirao, R. Kendall, J.A. Nichols, K. Tsemekhman, K. Wolinski, J. Anchell, D. Bernholdt, P. Borowski, T. Clark, D. Clerc, H. Dachsel, M. Deegan, K. Dyall, D. Elwood, E. Glendening, M. Gutowski, A. Hess, J. Jaffe, B. Johnson, J. Ju, R. Kobayashi, R. Kutteh, Z. Lin, R. Littlefield, X. Long, B. Meng, T. Nakajima, S. Niu, L. Pollack, M. Rosing, G. Sandrone, M. Stave, H. Taylor, G. Thomas, J. van Lenthe, A. Wong, Z. Zhang, NWChem, A Computational Chemistry Package for Parallel Computers, version 5.1, Pacific Northwest National Laboratory, Richland, WA, 2007.
- [19] C. Schlier, A. Seiter, *J. Phys. Chem. A* 102 (1998) 9399.
- [20] C. Schlier, A. Seiter, *Comput. Phys. Commun.* 130 (2000) 176.
- [21] T.-Y. Yan, C. Doubleday, W.L. Hase, *J. Phys. Chem. A* 108 (2004) 9863.
- [22] L. Yang, R. Sun, W.L. Hase, *J. Chem. Theory Comput.* 7 (2011) 3478.